Gold-Carbon Contacts from Oxidative Addition of Aryl Iodides

Rachel L. Starr,[†] Tianren Fu,[†] Evan A. Doud,[†] Ilana Stone,[†] Xavier Roy,*[,†] Latha Venkataraman*[,†,‡]

[†]Department of Chemistry, [‡]Department of Applied Physics and Mathematics, Columbia University, New York, New York 10027, United States

ABSTRACT: Aryl halide are ubiquitous functional groups in organic chemistry, yet despite their obvious appeal as surface-binding linkers and as precursors for controlled graphene nanoribbon synthesis, they have seldom been used as such in molecular electronics. The confusion regarding the bonding of aryl iodides to Au electrodes is a case in point, with ambiguous reports of both dative Au–I and covalent Au–C contacts. Here we form single-molecule junctions with a series of oligophenylene molecular wires terminated asymmetrically with iodine and thiomethyl to show that the dative Au–I contact has a lower conductance than the covalent Au–C interaction, which we propose occurs via an *in situ* oxidative addition reaction at the Au surface. Furthermore, we confirm the formation of the Au–C bond by measuring an analogous series of molecules prepared *ex situ* with the complex $Au^{I}(PPh_3)$ in place of the iodide. Density functional theory-based transport calculations support our experimental observations that Au–C linkages have higher conductance than Au–I linkages. Finally, we demonstrate selective promotion of the Au–C bond formation by controlling the bias applied across the junction. In addition to establishing the different binding modes of aryl iodides, our results chart a path to actively controlling oxidative addition on an Au surface using an applied bias.

INTRODUCTION

The controlled binding of single molecules between nanoscopic metal electrodes is a critical step in the design and assembly of molecular electronic devices. The specific binding groups, or linkers, on the molecule establish the mechanical connections to the electrodes and couple the discrete molecular orbitals to the electronic bands of the electrodes. Studying charge transport across the resulting metal-organic interfaces provides fundamental understanding of the nature of these contacts. Typical linkers used to bind organic molecules to metal electrodes include thiols,[1,2] thioethers,[3] and amines.[4] Although aryl halides are an extremely common and synthetically accessible functional group in organic chemistry, they have been used infrequently as linkers in molecular electronic applications. As a result, the binding motifs and electronic coupling strength of aryl halides are poorly understood. For example, some prior work with aryl iodides have reported dative Au–I contacts,[5,6] while others have suggested without substantial evidence that the iodide dissociates from the molecule, yielding a direct Au–C bond.[7] Such linkages are particularly attractive for single molecule electronics, as covalent interactions generally lead to an increase in conductance.[8] Junctions with Au–C linkages have been achieved using alkyne linkers[9,10,11] and trimethyl tin-functionalized precursors,[8,12,13] however these methods typically involve intensive syntheses, toxic chemicals, and are typically limited to select organic backbones. Aryl halides have also been used as precursors for the synthesis of graphene nanoribbons, an important component of next generation nanoscale electronic devices.[14] The dissociation of aryl halides is the first mechanistic step of this reaction, however the process only occurs under ultra-high vacuum and at high temperatures.[15]

In this work, we measure the single-molecule conductance of a series of asymmetric oligophenylene molecules with an iodide on one end and a thiomethyl group on the other. We demonstrate that the aryl iodide moiety undergoes a voltage-induced oxidative addition reaction on the Au surface to form a single molecule junction connected through a covalent Au–C bond. The formation of the Au–C bond is validated by measuring the conductance of the molecules *in situ* and comparing these values to control compounds prepared *ex situ* with the complex $Au^{I}(PPh_3)$ in place of the iodide. Our experimental measurements and supporting transport calculations based on density functional theory (DFT) reveal that junctions formed via Au–C bonds display an increased conductance when compared to junctions formed through a dative Au–I interaction. Moreover, we show that the proposed surface-based oxidative addition mechanism can be modulated by applying a voltage, wherein one electrode is polarized to increase its chemical potential, selectively promoting the reaction.

RESULTS AND DISCUSSION

Conductance measurements were carried out using the scanning tunneling microscope-based break junction (STM-BJ) technique[2,4] using solutions of the molecules in 1,2,4-trichlorobenzene (TCB, a non-polar solvent) or propylene carbonate (PC, a polar solvent). For the PC measurements, the Au tip was coated with an insulating layer to suppress background ionic current.[16] One dimensional (1D) conductance histograms and two-dimensional (2D) conductance-displacement histograms are constructed by compiling thousands of traces into logarithmic (conductance) and linear (displacement) bins without any data selection (see SI for details).

We first examine molecules in the series **1**-**4** comprising 1-4 phenylene units with asymmetric thiomethyl and iodide

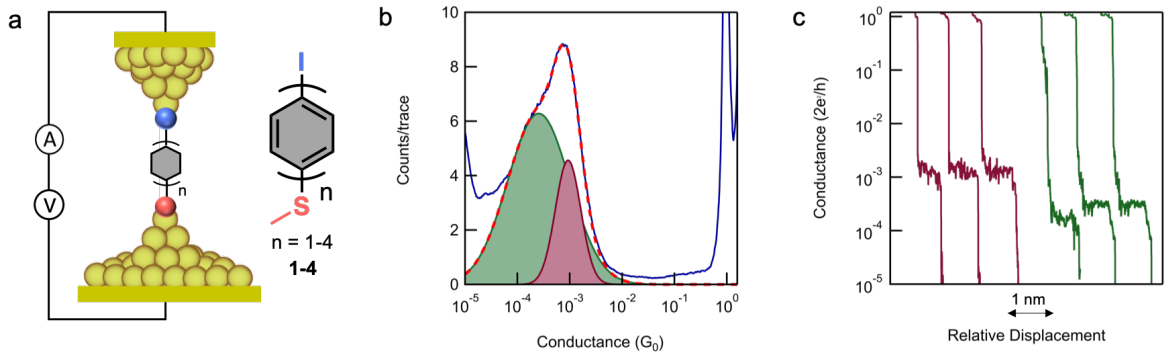

Figure 1. (a) Schematic of a single molecule junction and structure of **1-4**. (b) Logarithm-binned 1D histogram of **3** showing two peaks (taken at 100 mV in TCB). The histogram is fit with a double Gaussian (red), which is divided into high-G (magenta) and low-G (green) constituents. (c) Individual traces demonstrating the different conductance values corresponding to the high-G and low-G peaks.

linkers (Figure 1a). These molecules were synthesized using an iterative Suzuki cross-coupling strategy followed by functional group modification (see SI for synthetic details). The asymmetry of the linkers allows us to specifically probe the behavior of the iodide. Figure 1b highlights conductance data taken in TCB at 100 mV for **3** (see Figure S2 for the complete series). At all biases, there are two conductance states, suggesting the presence of two binding modes. The distinct conductance signatures are evidenced by a double peak in the 1D histogram (Figure 1b), and two plateaus of similar lengths in the individual traces (Figure 1c). The high- and low-conductance values (high- and low-G, respectively), extracted from the 1D histogram by fitting with a double Gaussian to these data, are 2.5×10^{-4} and 1.0×10^{-3} G_0 for **3**. Analogous analyses for **1**, **2** and **4** are in Figure S2.

These two different conductance states are remarkable, and cannot be attributed to two molecules in parallel given the factor of ~4 difference in conductance. Since we predominantly see either the high-G or the low-G, we can also rule out a simple junction conformational change that occurs upon elongation seen for analogous backbones with pyridine terminations.[17] We therefore hypothesize that the two conductance states arise from two distinct binding modes of the molecule in the junction: the low-G peak corresponds to molecules binding through a dative Au–I bond, and the high-G peak to molecules binding through a covalent Au–C bond, which forms through an oxidative addition of the aryl iodide to an undercoordinated Au atom at the electrode surface (Figure 2a). This hypothesis also rationalizes our observation that for each molecule, the length of the plateaus is consistent with the molecular length. We ascribe the low-G component of the double Gaussian fit to the Au–I interaction (Figure 1b, green) and the high-G component to the Au–C interaction (magenta). The dative Au–I interaction leads to a wider distribution of conductance values due to the many possible binding geometries and increased degrees of freedom of the aryl–I–Au contact. Symmetric molecules with two iodide linkers were also studied (Figure S3), but these yield more complicated data due to the multiple possible combinations of iodide dissociation.

To substantiate this hypothesis, we synthesized a new series of molecules (see SI for synthetic details) with an intrinsic Au–C bond in which the iodide linker present in **1-3** is replaced by a $Au^{I}(PPh_3)$ complex (Figure 2b, **Au1-Au3**).[11,18] Based on the propensity of the PPh_3 ligand to dissociate from the Au atom in the junction,[8] we conclude that **Au1-Au3** form molecular junctions analogous to those created with **1-3** upon Au–C bond formation. We first discuss **Au3** in relation to **3** (Figure 2c-e), and note that our observations apply to the complete series (Figure S4). Conductance measurements on **Au3**, performed under the same conditions as **3**, reveal only one conductance state whose position aligns with the high-G peak of **3**. The conductance value for **Au3**, obtained from a Gaussian fit of the peak, is in good agreement with the high-G of **3** (Figure 2c). Moreover, the conductance plateau of **Au3** in the 2D histogram (Figure 2e) has essentially the same shape and position as the high-G plateau of **3** (Figure 2d). We note that the plateau length of **Au3** is slightly longer than that of **3**, likely due to the extra Au atom (Figure S4 for entire series), as has been previously observed in analogous measurements.[19] These observations strongly support that **Au3** and the high-G conductance state of **3** are the same molecule in the junction.

The conductance values determined from both series, **1-4** and **Au1-Au3**, are plotted as a function of the molecular length (expressed as the number of phenylene units) on a semi-logarithmic scale (Figure 2f). From a linear fit of this data, we obtain the slope β, where $G \sim e^{-\beta n}$ describing the exponential decay of conductance with increasing number of phenylene units. The low-G state of **1-4** has a β value of 1.5 per phenylene unit, in good agreement with oligophenylene systems with dative linkers[20,21]. The β value for the high-G state of **1-4** is close to that of the **Au1-Au3** series and is smaller (1.2 per phenylene unit). This reinforces our conclusion that two distinct types of binding are occurring. Together, these observations confirm our hypothesis that the iodide dissociates in the junction, and a higher-conducting covalent Au–C linkage forms via oxidative addition. We theorize that the undercoordinated Au atoms at the junction, which are electron rich and reactive, promote the dissociation of the iodide by transferring electron density to the aryl carbon, enabling the formation the Au–C bond.

To understand these results, we turn to DFT to model the transmission across the molecular junctions using the FHI-aims package[22,23] and the AITRANSS code.[24,25] The modeled molecule in the junction is bound to the apex atoms of two 60-atom tetrahedral Au clusters that represent the electrodes. The transmission functions for **1-4** and **Au1-Au4** are calculated using the non-equilibrium Green's function formalism[24,25] starting from junction geometries optimized using the PBE exchange-correlation functional[26] (Figure 3a). The calculated molecular junction conductance of **2-4**, which is proportional

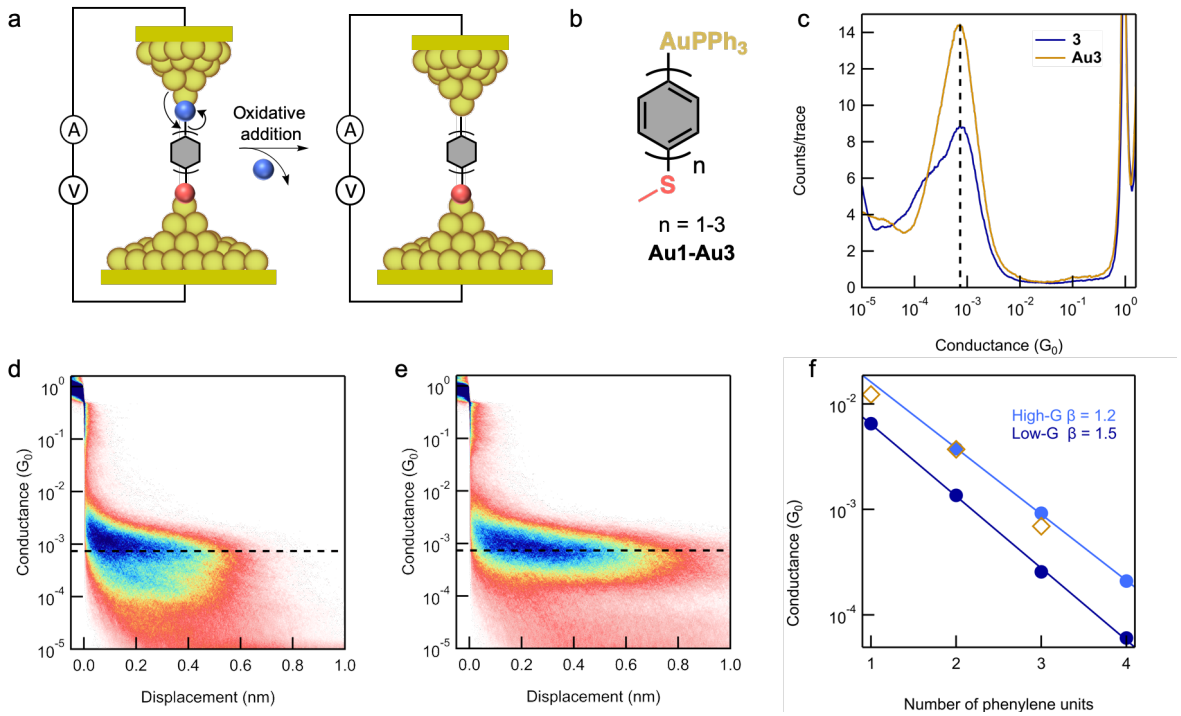

Figure 2. (a) Schematic of oxidative addition in the junction. (b) Structure of **Au1**-**Au3**. (c) 1D histograms of **3** (blue) and **Au3** (yellow). The black dashed line is a guide for the eye denoting the high-G conductance value of **3**, and aligning with the peak conductance value for **Au3**. (d) 2D histogram of **3** (TCB, 100 mV), with the black dashed line denoting the high-G conductance value. (e) 2D histogram of **Au3** (TCB, 100 mV), with the same black dashed line denoting the **3** high-G conductance value aligning with the **Au3** peak conductance. The longer plateau is consistent with an extra Au atom in the junction. (f) Semi-logarithmic plot of the conductance histogram peak value as a function of the number of phenylene units in the backbone of **1**-**4** (filled circles) and **Au1**-**Au3** (unfilled diamonds). The **Au1**-**Au3** peak values align with the high-G values of **1**-**4**. β values are calculated from the linear fit.

to the transmission at the Fermi level (E_F), is lower than that of **Au2**-**Au4**, with the difference in conductance increasing with molecular length. This trend reproduces the experimental results shown in Figure 2f. Figure 3b shows the transmission at E_F of **1**-**4** and **Au1**-**Au4** plotted against molecule length. This data is fit to an exponential function $T = Ae^{-\beta n}$ to obtain the conductance decay for the series. The β value obtained from the fit of the **1**-**4** series (0.69 per phenylene unit) is larger than that of the **Au1**-**Au4** series (0.58 per phenylene unit), also in agreement with the experimental observations (Figure 3b). These calculations provide further support to our hypothesis that the iodide dissociates during junction formation resulting in an Au–aryl linkage.

The DFT-based calculations discussed above overestimate the conductance[27] because the PBE exchange-correlation functional underestimates the molecular HOMO-LUMO gaps. To examine this limitation, we repeated the calculation using B3LYP functional, which yields more accurate HOMO-LUMO gaps but is computationally expensive. We modeled **2** and **Au2** attached to 18 Au atom clusters as model electrodes and find that for both junctions, the HOMO-LUMO gap is larger and the transmission at E_F calculated using the B3LYP functional is lower than those calculated using PBE (Figure S5).[28–30] Note that DFT does not include the polarizability of metal in response to charge transfer, implying that B3LYP overestimates the energy separation between the HOMO and LUMO resonances in

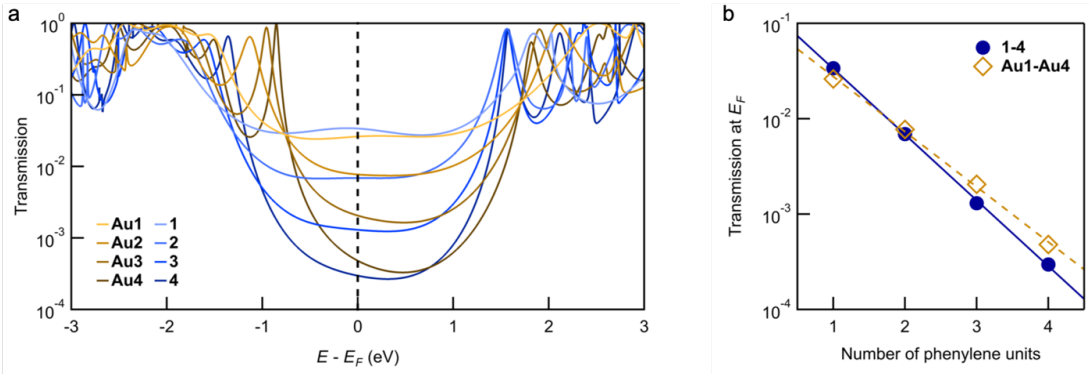

Figure 3. (a) Calculated transmission functions of **1**-**4** and **Au1**-**Au4**. (b) Calculated transmission at E_F plotted against molecule length, demonstrating the decay is different for each series (**1**-**4**: β = 0.69 per phenylene unit; **Au1**-**Au4**: β = 0.58 per phenylene unit).

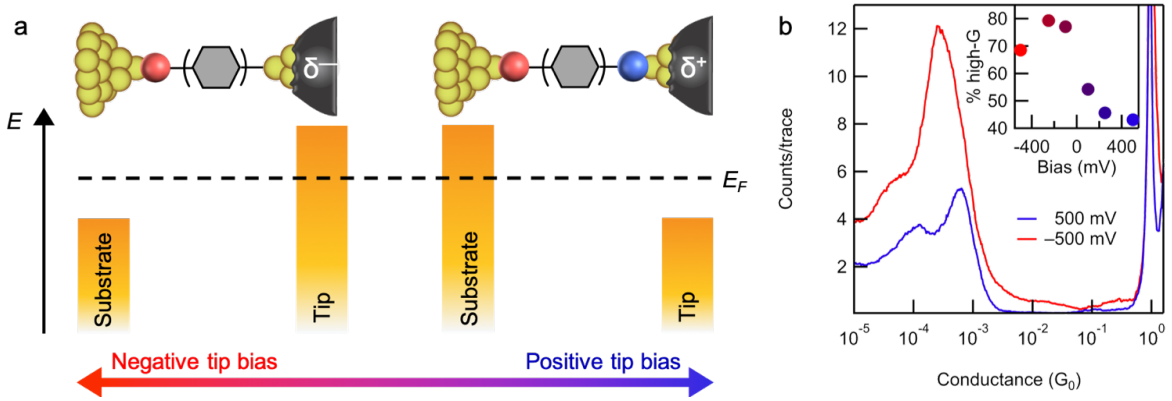

Figure 4. (a) Schematic of a single-molecule junction created in an ionic environment, using a wax-coated tip. When a positive tip bias is applied (right, denoted by δ+), Au–I linkages are favored. When a negative tip bias is applied (left, denoted by δ–), electron density at the tip can be donated to the aryl carbon, favoring the direct Au–C linkage. (b) 1D histograms taken in PC at ± 500 mV, demonstrating preferential Au–C junction formation at negative bias. Inset: percentage of junctions that are Au–C compared to Au–I.

the transmission function.[31] We may thus regard the PBE and B3LYP results as upper and lower bounds of the transmission function, respectively. The transmission of **Au2** is about two-fold higher than **2** at E_F according to PBE and ten-fold according to B3LYP. This again fits the experimental trends.

When measured in TCB, the 1D and 2D histograms of **1**-**4** consistently show conductance features indicative of both dative Au–I and covalent Au–C linkages. We now demonstrate that the formation of the Au–C linkage can be actively favored by using an electrical bias to modulate the chemical potential of the electrode. These measurements are performed with a wax-coated tip in the polar solvent PC with tetrabutylammonium hexafluorophosphate ($TBAPF_6$, 100 mM concentration) as a supporting electrolyte. This setup allows us to polarize the tip electrode through the formation of a dense double layer of charge at the small exposed area.[32] Figure 4a illustrates how the application of a negative bias increases the chemical potential of the tip, making it electron rich, therefore promoting the oxidative addition reaction that leads to the Au–C bond formation.

To examine this possibility, we measured **3** at various applied tip biases between –500 and 500 mV. All 1D histograms show both low-G and high-G peaks (Figure S6), indicating that both Au–I and Au–C bound junctions form. The relative height of these two peaks, however, changes dramatically with bias. This is illustrated in Figure 4b for tip biases of –500 and 500 mV. Note that the peaks shift as a result of the applied bias due to a gating effect.[33] At 500 mV, the height of the two peaks is similar, signifying that both Au–I and Au–C bound junctions are equally probable. At –500 mV the high-G peak is much more prominent, demonstrating that Au–C bound junctions form much more frequently than Au–I bound ones at negative bias.

To quantify the effect of the applied bias, we analyze our traces to determine the percentage of high-G traces in a given data set (Figure S6). The average percentage of high-G at each bias is shown in the inset of Figure 4b. The percentage of high-G traces gradually increases as the bias changes from 500 to –500 mV, essentially doubling from around 40% to 80% within this bias range. At positive bias, the tip is electron deficient, and both Au–I and Au–C interactions are present while at negative bias, the tip is electron rich and thus more prone to undergo oxidative addition with the aryl iodide moiety to form the Au–C bond.

CONCLUSION

By studying a series of asymmetric oligophenylene compounds, we have established two different binding modes of aryl iodide linkers to Au electrodes in single-molecule junctions. We observe both a lower-conducting, dative Au–I contact and a higher-conducting, covalent Au–C bond. Our data indicate that the Au–C bond forms through an oxidative addition process, in which the electron rich Au electrode enables iodide dissociation. Remarkably, this reaction can be controlled by the applied tip bias. This leads to desirable, higher-conducting covalent Au–C linkages that were previously accessible only through complicated methods. This work opens the door to manipulating chemical transformations using the electric field generated in the molecular junction.

ASSOCIATED CONTENT

Supporting Information

The Supporting Information is available free of charge on the ACS Publications website.

Synthetic details, characterization, DFT calculations, STM-BJ experimental details, and additional data (PDF)

AUTHOR INFORMATION

Corresponding Authors

lv2117@columbia.edu
xr2114@columbia.edu

Author Contributions

The manuscript was written through contributions of all authors. All authors have given approval to the final version of the manuscript.

ACKNOWLEDGMENTS

Experimental work was supported primarily by the National Science Foundation award grant CHE-1807654 and CAREER Award DMR-1751949. T.F. is supported by the NSF Graduate Research Fellowship under grant CHE-1764256. We thank María Camarasa-Gómez and Ferdinand Evers for assistance with DFT calculations.

Mass spectrometry was carried out by Brandon Fowler, and cyclic voltammetry by Jake Russell.

REFERENCES

(1) Reed, M. A.; Zhou, C.; Muller, C. J.; Burgin, T. P.; Tour, J. M. Conductance of a Molecular Junction. *Science.* **1997**, *278*, 252–255.

(2) Xu, B.; Tao, N. J. Measurement of Single-Molecule Resistance by Repeated Formation of Molecular Junctions. *Science.* **2003**, *301*, 1221–1224.

(3) Park, Y. S.; Whalley, A. C.; Kamenetska, M.; Steigerwald, M. L.; Hybertsen, M. S.; Nuckolls, C.; Venkataraman, L. Contact Chemistry and Single-Molecule Conductance : A Comparison of Phosphines , Methyl Sulfides , and Amines. *J. Am. Chem. Soc.* **2007**, *129*, 15768–15769.

(4) Venkataraman, L.; Klare, J. E.; Nuckolls, C.; Hybertsen, M. S.; Steigerwald, M. L. Dependence of Single-Molecule Junction Conductance on Molecular Conformation. *Nature* **2006**, *442*, 904–907.

(5) Komoto, Y.; Fujii, S.; Hara, K.; Kiguchi, M. Single Molecular Bridging of Au Nanogap Using Aryl Halide Molecules. *J. Phys. Chem. C* **2013**, *117*, 24277–24282.

(6) Peng, L.; Huang, B.; Zou, Q.; Hong, Z.; Zheng, J.; Shao, Y.; Niu, Z.; Zhou, X.; Xie, H.; Chen, W. Low Tunneling Decay of Iodine-Terminated Alkane Single-Molecule Junctions. *Nanoscale Res. Lett.* **2018**, *13*, 121–126.

(7) Zhou, G.; Tao, N.; Asai, Y. The Orbital Selection Rule for Molecular Conductance as Manifested in Tetraphenyl-Based Molecular Junctions. *J. Am. Chem. Soc.* **2017**, *139*, 2989–2993.

(8) Cheng, Z.; Skouta, R.; Vazquez, H.; Widawsky, J. R.; Schneebeli, S.; Chen, W.; Hybertsen, M. S. In Situ Formation of Highly Conducting Covalent Au–C Contacts for Single-Molecule Junctions. *Nat. Nanotechnol.* **2011**, *6* (6), 353–357.

(9) Hong, W.; Li, H.; Liu, S.; Fu, Y.; Li, J.; Kaliginedi, V.; Decurtins, S.; Wandlowski, T. Trimethylsilyl-Terminated Oligo(Phenylene Ethynylene)s: An Approach to Single-Molecule Junctions with Covalent Au−C Σ-Bonds. *J. Am. Chem. Soc.* **2012**, *134* (47), 19425–19431.

(10) Bejarano, F.; Olavarria-contreras, I. J.; Droghetti, A.; Rungger, I.; Rudnev, A.; Gutiérrez, D.; Mas-torrent, M.; Veciana, J.; van der Zant, H. S. J.; Rovira, C.; Burzurí, E.; Crivillers, N. Robust Organic Radical Molecular Junctions Using Acetylene Terminated Groups for C−Au Bond Formation. *J. Am. Chem. Soc.* **2018**, *140*, 1691–1696.

(11) Millar, D.; Venkataraman, L.; Doerrer, L. H. Efficacy of Au - Au Contacts for Scanning Tunneling Microscopy Molecular Conductance Measurements. *J. Phys. Chem. C* **2007**, *111* (47), 17635–17639.

(12) Batra, A.; Kladnik, G.; Gorjizadeh, N.; Steigerwald, M.; Nuckolls, C.; Quek, S. Y.; Cvetko, D.; Morgante, A.; Venkataraman, L. Trimethyltin-Mediated Covalent Gold − Carbon Bond Formation. *J. Am. Chem. Soc.* **2014**, *136* (36), 12556–12559.

(13) Chen, W.; Widawsky, J. R. Highly Conducting π -Conjugated Molecular Junctions Covalently Bonded to Gold Electrodes. *J. Am. Chem. Soc.* **2011**, *133* (43), 17160–17163.

(14) Cai, J.; Ruffieux, P.; Jaafar, R.; Bieri, M.; Braun, T.; Blankenburg, S.; Muoth, M.; Seitsonen, A. P.; Saleh, M.; Feng, X.; Müllen, K.; Fasel, R. Atomically Precise Bottom-up Fabrication of Graphene Nanoribbons. *Nat. Lett.* **2010**, *466*, 470–473.

(15) Batra, A.; Cvetko, D.; Kladnik, G.; Adak, O.; Cardoso, C.; Ferretti, A.; Prezzi, D.; Molinari, E.; Morgante, A.; Venkataraman, L. Probing the Mechanism for Graphene Nanoribbon Formation on Gold Surfaces through X-Ray Spectroscopy. *Chem. Sci.* **2014**, *5*, 4419–4423.

(16) Nagahara, L. A.; Thundat, T.; Lindsay, S. M. Preparation and Characterization of STM Tips for Electrochemical Studies. *Rev. Sci. Instrum.* **1989**, *60* (10), 3128–3130.

(17) Quek, S. Y.; Kamenetska, M.; Steigerwald, M. L.; Choi, H. J.; Louie, S. G.; Hybertsen, M. S.; Neaton, J. B.; Venkataraman, L. Mechanically Controlled Binary Conductance Switching of a Single-Molecule Junction. *Nat. Nanotechnol.* **2009**, *4*, 230–234.

(18) Pankajakshan, S.; Loh, T. Base-Free Palladium-Catalyzed Sonogashira Coupling Using Organogold Complexes. *Chem. Asian J.* **2011**, *6*, 2291–2295.

(19) Inkpen, M. S.; Liu, Z. F.; Li, H.; Campos, L. M.; Neaton, J. B.; Venkataraman, L. Non-Chemisorbed Gold–Sulfur Binding Prevails in Self-Assembled Monolayers. *Nat. Chem.* **2019**, *11*, 351–358.

(20) Zang, Y.; Pinkard, A.; Liu, Z.; Neaton, B.; Steigerwald, M. L.; Roy, X.; Venkataraman, L. Electronically Transparent Au − N Bonds for Molecular Junctions. *J. Am. Chem. Soc.* **2017**, *139*, 14845–14848.

(21) Hsu, L.; Wu, N.; Rabitz, H. Conductance and Activation Energy for Electron Transport in Series and Parallel Intramolecular Circuits. *Phys. Chem. Chem. Phys.* **2016**, *18*, 32087–32095.

(22) Blum, V.; Gehrke, R.; Hanke, F.; Havu, P.; Havu, V.; Ren, X.; Reuter, K.; Scheffler, M. Ab Initio Molecular Simulations with Numeric Atom-Centered Orbitals. *Comput. Phys. Commun.* **2009**, *180* (11), 2175–2196.

(23) Havu, V.; Blum, V.; Havu, P.; Scheffler, M. Efficient O(N) Integration for All-Electron Electronic Structure Calculation Using Numeric Basis Functions. *J. Comput. Phys.* **2009**, *228* (22), 8367–8379.

(24) Arnold, A.; Weigend, F.; Evers, F. Quantum Chemistry Calculations for Molecules Coupled to Reservoirs : Formalism , Implementation , and Application to Benzenedithiol Formalism , Implementation , and Application to Benzenedithiol. *J. Chem. Phys.* **2007**, *126*, 174101.

(25) Bagrets, A. Spin-Polarized Electron Transport Across Metal−Organic Molecules: A Density Functional Theory Approach. *J. Chem. Theory Comput.* **2013**, *9*, 2801–2815.

(26) Perdew, J. P.; Burke, K.; Ernzerhof, M. Generalized Gradient Approximation Made Simple. *Phys. Rev. Lett.* **1996**, *77* (18), 3865–3868.

(27) Koentopp, M.; Burke, K.; Evers, F. Zero-Bias Molecular Electronics : Exchange-Correlation Corrections to Landauer's Formula. *Phys. Rev. B* **2006**, *73*, 121403.

(28) Vosko, S.; Wilk, L.; Nusair, M. Accurate Spin-Dependent Electron Liquid Correlation Energies for Local Spin Density Calculations: A Critical Analysis1. *Can. J. Phys.* **1980**, *58*, 1200.

(29) Lee, C.; Yang, W.; Parr, R. G. Development of the Colle-Salvetti Correlation-Energy Formula into a Functional of the Electron Density. *Phys. Rev. B* **1988**, *37* (2), 785–789.

(30) Becke, A. D. A New Mixing of Hartree–Fock and Local Density-Functional Theories. *J. Chem. Phys.* **1993**, *98*, 1372.

(31) Egger, D. A.; Liu, Z.; Kronik, L. Reliable Energy Level Alignment at Physisorbed Molecule − Metal Interfaces from Density Functional Theory. *Nano Lett.* **2015**, *15*, 2448–2455.

(32) Capozzi, B.; Xia, J.; Adak, O.; Dell, E. J.; Liu, Z.; Taylor, J. C.; Neaton, J. B.; Campos, L. M.; Venkataraman, L. Single-Molecule Diodes with High Recti Fi Cation Ratios through Environmental Control. *Nat. Nanotechnol.* **2015**, *10*, 522–527.

(33) Capozzi, B.; Low, J. Z.; Xia, J.; Liu, Z.-F.; Neaton, J. B.; Campos, L. M.; Venkataraman, L. Mapping the Transmission Functions of Single-Molecule Junctions. *Nano Lett.* **2016**, *16* (6), 3949–3954.

Insert Table of Contents artwork here